

## Precision Measurement of the Hyperfine Structure of Laser-Cooled Radioactive ${}^7\text{Be}^+$ Ions Produced by Projectile Fragmentation

K. Okada,<sup>1</sup> M. Wada,<sup>2,3,\*</sup> T. Nakamura,<sup>2</sup> A. Takamine,<sup>2</sup> V. Lioubimov,<sup>2,8</sup> P. Schury,<sup>2</sup> Y. Ishida,<sup>2</sup> T. Sonoda,<sup>2</sup> M. Ogawa,<sup>4</sup> Y. Yamazaki,<sup>2,4</sup> Y. Kanai,<sup>2</sup> T. M. Kojima,<sup>2</sup> A. Yoshida,<sup>3</sup> T. Kubo,<sup>3</sup> I. Katayama,<sup>5</sup> S. Ohtani,<sup>6</sup> H. Wollnik,<sup>7</sup> and H. A. Schuessler<sup>8</sup>

<sup>1</sup>Department of Physics, Sophia University, 7-1 Kioicho, Chiyoda, Tokyo 102-8554, Japan

<sup>2</sup>Atomic Physics Laboratory, RIKEN, 2-1 Hirosawa, Wako, Saitama 351-0198, Japan

<sup>3</sup>Nishina Center for Accelerator Based Science, RIKEN, 2-1 Hirosawa, Wako, Saitama 351-0198, Japan

<sup>4</sup>Graduate School of Arts and Science, The University of Tokyo, Meguro, Tokyo 153-8902, Japan

<sup>5</sup>Institute of Particle and Nuclear Studies, High Energy Accelerator Research Organization (KEK), Tsukuba, Ibaraki 305-0801, Japan

<sup>6</sup>Institute for Laser Science (ILS), University of Electro-Communications, 1-5-1 Chofugaoka, Chofu, Tokyo, 182-8585, Japan

<sup>7</sup>II. Physikalisches Institut, Justus-Liebig-Universität Giessen, Giessen, Germany

<sup>8</sup>Department of Physics, Texas A&M University, College Station, Texas 77843, USA

(Received 20 June 2008; published 18 November 2008)

The ground state hyperfine splitting of  ${}^7\text{Be}^+$  has been measured by laser-microwave double-resonance spectroscopy in the online rf trap of RIKEN's slow RI-beam facility. Be ions produced by projectile fragmentation of  ${}^{13}\text{C}$  at  $\approx 1$  GeV were thermalized in a rf ion guide gas cell and subsequently laser cooled in the ion trap to  $\approx 1$   $\mu\text{eV}$ . This  $10^{15}$ -fold reduction of the kinetic energy allows precision spectroscopy of these ions. A magnetic hfs constant of  $A = -742.772\,28(43)$  MHz was measured for  ${}^7\text{Be}^+$ , from which a nuclear magnetic moment of  $\mu_I = -1.399\,28(2)\mu_N$  was deduced.

DOI: 10.1103/PhysRevLett.101.212502

PACS numbers: 21.10.Ky, 27.20.+n, 31.30.Gs, 37.10.Ty

Optical atomic spectroscopy of unstable nuclei has played an important role in nuclear structure studies [1,2]. Nuclear charge radii and moments for many unstable nuclei were determined model-independently by optical spectroscopy of low energy ion beams or stored ions. The number of nuclides available for investigation by optical spectroscopy has been restricted to about 500 nuclei of about 50 elements [2], mostly limited by low energy radioactive ion beams available at conventional isotope-separator-online (ISOL) facilities. The present experiment at the new slow radioactive ion (SLOWRI) facility at RIKEN opens up a new frontier. It uses radioactive ions produced by fragmentation at relativistic energies and reduces them to subthermal energies. Simultaneously the method is fast, chemistry independent, and the in-flight separation in a fragment separator is capable of producing any isotope.

While  $\text{Be}^+$  ions are becoming available at ISOL facilities due to advances in laser ion sources, our universal method quickly and efficiently provides low energy radioactive ion beams of all elements by combining a projectile fragment separator with a gas stopper and also utilizing a rf-carpet ion guide [3,4]. In the future it promises that more than 4000 unexplored nuclei will be available for study. We demonstrate here, for the first time, both laser cooling [5] and precision hfs spectroscopy of radioactive ions from projectile fragmentation, and have selected  $\text{Be}^+$  as the first candidate.

${}^7\text{Be}$  is a unique nucleus whose nuclear moments elude determination by the  $\beta\gamma$ -NMR method [6], since it emits

no  $\beta$  rays and emits  $\gamma$  rays isotropically. Optical spectroscopy is therefore the only way to measure the nuclear moments. Earlier, the hfs of  ${}^7\text{Be}^+$  was *indirectly* observed by collinear fast beam laser spectroscopy with limited accuracy and reported in [7]. At SLOWRI, we recently have *directly* measured the hfs of  ${}^7\text{Be}^+$  with an accuracy of  $5 \times 10^{-7}$  by laser-microwave double-resonance (LMDR) spectroscopy. This is the first step towards an investigation of the neutron halo nucleus  ${}^{11}\text{Be}$  through observation of the Bohr-Weisskopf effect [8], which could test the predicted extended distribution of a valence neutron by employing a purely electromagnetic probe [9].

The hyperfine structure and the hyperfine field of the Be ion have been theoretically investigated with high accuracy [10,11]. The effect of nuclear structure, however, is not clearly known as only the stable isotope  ${}^9\text{Be}^+$  has been experimentally studied so far [12–14]. Our present measurement of ions of the isotope  ${}^7\text{Be}$  allows separation of the nuclear and mass dependent contribution to the hfs for more stringent comparisons with theory.

Laser cooling is an essential prerequisite to measure the hfs constant of  $\text{Be}^+$  by LMDR spectroscopy, since otherwise the hfs splitting ( $\sim 1$  GHz) is too small to be resolved, particularly since the Doppler width of the  $2s^2S_{1/2} \rightarrow 2p^2P_{1/2,3/2}$  transition is  $\sim 5$  GHz at room temperature. Circularly polarized laser radiation at a frequency slightly lower than the resonance can achieve both optical pumping into a recyclable state and laser cooling. The atomic ground state of  ${}^7\text{Be}^+$  is split into two hfs levels of  $F = \{2, 1\}$ , and the excited  ${}^2P_{3/2}$  state is split into four hfs levels

of  $F = \{3, 2, 1, 0\}$ , if a nuclear spin  $I = 3/2$  is assumed. In the presence of a magnetic field of about 0.6 mT the ground state hfs levels further split into Zeeman levels described by  $m_F$  while the excited  $2p^2P_{3/2}$  state already splits into Paschen-Back levels described by  $(m_I, m_J)$  (Fig. 1). When  $\sigma^+$  radiation excites the  $2s^2S_{1/2} \rightarrow 2p^2P_{3/2}$  transition, the level population of the ground state quickly shifts to the larger  $m_F$  states, concentrating in the maximum  $m_F$  state,  $(F, m_F) = (2, +2)$ , while the excited state concentrates in the maximum  $m_J + m_I$  state  $(m_J, m_I) = (+3/2, +3/2)$ . Once such optical pumping is achieved, closed cycling of excitation and deexcitation between these levels is repeated, resulting in efficient laser cooling. It should be noted that the population in the  $F = 1$  hyperfine level of the ground state is also gradually pumped into the  $(F, m_F) = (2, +2)$  state by the laser excitation initially via Doppler broadening and finally via the Lorentzian wing of the resonance line.

A single laser-cooled ion radiates photons via laser-induced fluorescence (LIF) at the high rate of  $\approx 10^6 \text{ s}^{-1}$ , allowing sensitive observation with only a few radioactive ions in the trap. If in addition an M1 transition from the pumped state to the other hfs state of ground state  $[(F, m_F) = (2, +2) \rightarrow (1, +1)]$  is induced by resonant microwave radiation, a leak from the closed cycle occurs and the strong LIF is reduced until a repumping process takes place. In this way, the microwave resonance of the hfs splitting can be observed with high sensitivity as a dip in the LIF intensity spectrum as a function of the microwave frequency. Previously, we have detailed the procedure of the LMDR method in the case of  $^9\text{Be}^+$  [13].

From the two observed microwave resonance frequencies,  $\nu^+$  and  $\nu^-$ , corresponding to the polarization of the laser radiation,  $\sigma^+$  and  $\sigma^-$ , the magnetic hfs constant  $A$  can be deduced using the Breit-Rabi formula. The sign of  $A$  is the sign of the nuclear magnetic moment  $\mu_I$  and is determined from the comparison of  $\nu^+$  with  $\nu^-$ . The nuclear spin  $I$  is determined from the magnetic field dependence of  $\nu$ .

The experiment was performed at the prototype SLOWRI facility at RIKEN. A 100A-MeV  $^{13}\text{C}$  beam

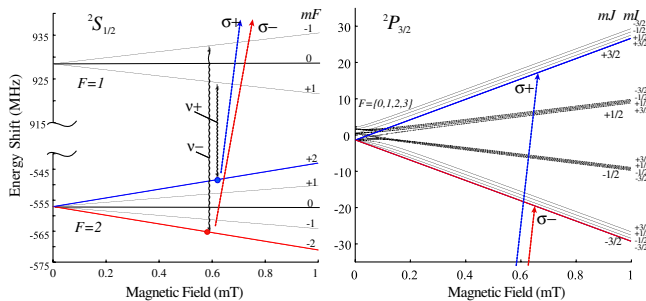


FIG. 1 (color online). Atomic level diagram of the ground  $2s^2S_{1/2}$  state and the excited  $2p^2P_{3/2}$  state of  $^7\text{Be}^+$  with magnetic field dependence.

from the RIKEN ring cyclotron impinged a 5 mm-thick Be metal target, producing nuclei of many isotopes, including  $^7\text{Be}$ , by a fragmentation reaction.  $^7\text{Be}$  ions are then separated by the RIKEN projectile fragment separator RIPS [15]. After energy reduction to less than  $2A$  MeV in an energy degrader, the Be ions are injected into a gas-catcher cell filled with 26 hPa helium gas. In the gas cell the Be ions are thermalized, and guided to a small exit nozzle by a rf-carpet [3]. The extracted ions are transported to an ultrahigh vacuum chamber by a 600-mm-long octupole ion beam guide (OPIG) made of a carbon fiber reinforced plastic material through three differential pumping sections. Various kinds of contaminant ions, mainly molecules originating in the gas cell, are also transported through the OPIG. They are filtered by a quadrupole mass filter placed behind the OPIG. The resolution of the filter is about 0.5 amu which is sufficient to eliminate contaminant ions. The purified  $^7\text{Be}^+$  ions are injected into a cryogenic linear rf trap for precision spectroscopy. In order to accumulate  $^7\text{Be}^+$  ions from the continuous beam with a few eV energy, 10 mPa He gas is loaded into the spectroscopy chamber during the ion accumulation period of about 10 s.

The central part of the linear rf trap is shown in Fig. 2. The trap electrodes are made of 10 mm diameter rods of SUS316 and are arranged in a quadrupole configuration having an inner radius of  $r_0 = 4.35$  mm. The linear trap is segmented into three sections, and end-plate electrodes at higher potential are attached to both ends to axially confine the  $^7\text{Be}^+$  ions. The total and the center section lengths of the trap are 97 and 20 mm, respectively. The trap electrodes, the radiation shields, and the He gas pipe are thermally connected to a 10 K cold refrigeration sink to reduce all gas impurities.

A 313 nm cw laser setup [5,13,14] was located 50 m away from the ion trap on another floor. A pair of telescopes and several mirrors were used to transport and focus the radiation into the trap. The circular polarization was maintained by a Glan-Taylor prism and a  $\lambda/4$  wave plate placed just in front of the trap chamber. The polarization

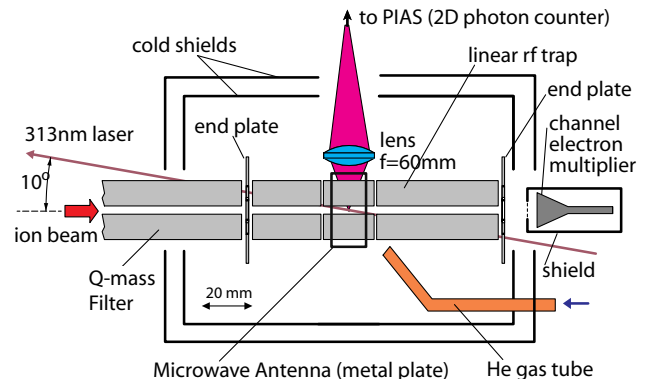


FIG. 2 (color online). Schematic drawing of the center part of the experimental setup.

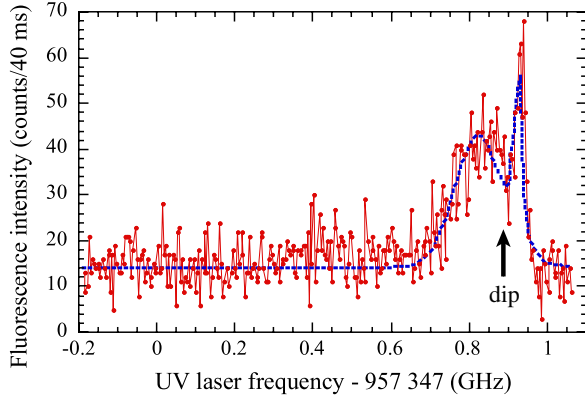


FIG. 3 (color online). Laser-cooling spectrum of  ${}^7\text{Be}^+$ . The horizontal axis shows the absolute uv laser frequency calibrated by an optical frequency comb system. The symbols are data points and the curve guides the eye. The transition from a broad line shape to a sharp peak with a characteristic dip indicates that the so-called crystallization of  ${}^7\text{Be}^+$  ions occurred in the rf trap.

can be quickly switched ( $\sigma^+ \leftrightarrow \sigma^-$ ) by rotating the remotely controlled  $\lambda/4$  wave plate. The direction of the laser radiation was tilted by  $10^\circ$  with respect to the trap axis to avoid interference with the ion detector. A weak ( $\sim 0.6$  mT) magnetic field produced by Helmholtz-type coils was applied parallel to the laser radiation. The current of the coils was stabilized to  $10^{-5}$  by an accurate shunt resistor and a software feedback system. Two other pairs of coils were used to compensate stray magnetic fields to the few  $\mu\text{T}$  level.

For tuning the uv laser frequency to the  ${}^2S_{1/2} \rightarrow {}^2P_{3/2}$  transition, the fundamental laser wave length (626 nm) is monitored using a commercial wave meter. The absolute frequency was calibrated using an optical frequency comb system [16] and Doppler-free saturated absorption signals from an  $I_2$  cell. The laser was detuned by 200–300 MHz below the resonance of the  ${}^2S_{1/2} \rightarrow {}^2P_{3/2}$  transition, and was chopped at 7 kHz with a 90% duty factor by an electro-optic modulator during LMDR spectroscopy, to avoid any broadening and shifting in the microwave resonance. The typical average power of the laser radiation at the entrance of the chamber was 0.3 mW. The LIF signal was detected by a two dimensional photon-counting system (PIAS, Hamamatsu) through a lens and an interference filter. The photon detector was used not only for imaging the ion crystal but also to reduce the background by means of spacial filtering. Microwave radiation generated by a synthesizer and amplified by a traveling wave tube to about 0.5 W was introduced to an antenna placed close to the trap electrodes (Fig. 2). The microwave radiation was pulsed to irradiate only during the laser off periods.

Figure 3 shows the LIF spectrum of laser-cooled  ${}^7\text{Be}^+$  ions in the linear rf trap. The dip in the spectrum indicates that a phase transition from an ion-cloud state to an ion crystal state occurred [17]. The temperature of the ions can

be evaluated from the sharp peak at higher frequency to be less than 10 mK, corresponding to  $< 1 \mu\text{eV}$ —a  $10^{15}$ -fold reduction in the kinetic energy of the ions. This is a rapid shift from relativistic energies to quantum energies.

A typical microwave spectrum of the  $(F, m_F) = (2, +2) \rightarrow (1, +1)$  transition is shown in Fig. 4, fitted to a Gaussian profile to determine the resonance frequency. This is because the width of the resonance curve is considered to be due to the spacial inhomogeneity and short-term fluctuation of the magnetic field, and the amplitude of the peak varies very much depending on the optical pumping conditions while the center frequencies of the resonance remained unchanged within the statistical error. We performed several measurements of  $\nu^+$  and  $\nu^-$  at two different magnetic fields of 0.61 and 0.71 mT and the results are summarized in Table I. The sign of the hfs constant of  ${}^7\text{Be}^+$ ,  $A_7$  is confirmed to be negative from  $\nu^+ - \nu^- < 0$ . The magnetic field dependence of  $\nu^-$  can be described as  $d\nu/dB = \mu_B 4I/(2I + 1)$  where  $\mu_B = 14 \text{ MHz/mT}$ . The measured dependence was 21 MHz/mT which is consistent with the nuclear spin  $I = 3/2$ . The magnetic hfs constant  $A_7 = -742.772\,28(43) \text{ MHz}$  is determined from the four frequencies listed in Table I.

The nuclear magnetic moment of  ${}^7\text{Be}$  was deduced to be  $\mu_I({}^7\text{Be}) = -1.399\,28(2)\mu_N$  from the measured values of  $A_7$  and  $I_7$  with reference to the corresponding values of  ${}^9\text{Be}$  [ $A_9 = -625.008\,837\,048(10) \text{ MHz}$ ,  $\mu_I({}^9\text{Be}) = -1.177\,432(3)\mu_N$ ,  $I_9 = 3/2$ ] [12,18,19] by the relation of  $\mu_I({}^7\text{Be})/I_7 = (1 + \Delta_{7,9})(A_7/A_9)(\mu_I({}^9\text{Be})/I_9)$ , where the small differential hyperfine anomaly  $\Delta_{7,9}$  was neglected. The uncertainty of  $\mu_I({}^7\text{Be})$  is evaluated, however, from the theoretically derived magnitude of  $\Delta_{7,9} < 10^{-5}$  [9].

The experimental value was compared with theoretical calculations and some empirical calculations as shown in Table II. A simple shell model calculation with OXBASH using the Cohen-Kurath [20] interaction shows good agree-

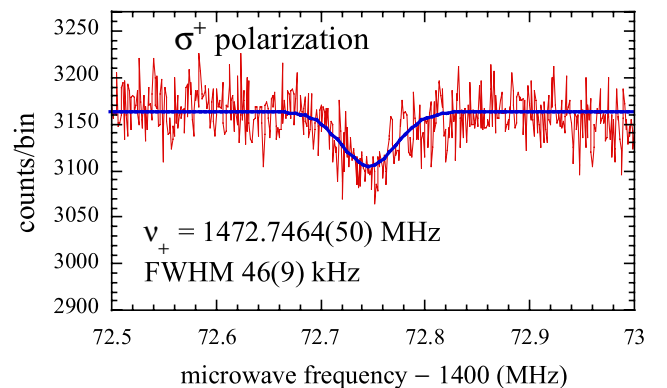


FIG. 4 (color online). Typical LMDR spectrum of the ground state hfs transitions of  $(F, m_F) = (2, +2) \rightarrow (2, +1)$  for  ${}^7\text{Be}^+$  ions at  $B = 0.610\,56(19) \text{ mT}$ .

TABLE I. Resonance frequencies  $\nu^+$  and  $\nu^-$  at two different magnetic fields. Each frequency is the result of the fitting from 3 or 4 measurements, and the magnetic fields are obtained together with the hfs constant  $A$  from the fitting of the four frequencies to the Breit-Rabi formula.

Quantity	$I_{\text{coil}} = 12 \text{ A}$	$I_{\text{coil}} = 14 \text{ A}$
$B$ (mT)	0.6106 1(13)	0.7127 7(4)
$\nu^+$ (MHz)	1472.745 4(32)	1470.613 1(13)
$\nu^-$ (MHz)	1498.413 8(46)	1500.577 1(13)

ment, with a 1.5% discrepancy, while the large-basis shell model calculation [21], the *ab initio* shell model calculation [22] by Navrátil *et al.*, and the variational quantum Monte Carlo calculations by Pudliner *et al.* [23] show large discrepancies of about 20%. These modern calculations achieved good agreement for the magnetic moments of  $T = 0$  isoscalar nuclei, such as  $^{10}\text{B}$ , but not for  $T = 1/2$  isovector nuclei. This is due to two-body charge and current contributions, which are not included in the calculations, and are greatly cancelled in the isoscalar nuclei, while they are noticeable in the isovector nuclei [25].

A prediction by an empirical linear relation between the nuclear  $g$  factors of mirror nuclei found by Buck *et al.* [24] showed good agreement in heavier mirror nuclei. However, a discrepancy of about 5% is seen in  $^7\text{Be}$ .

An accurate prediction comes from the relation between the isospin doublet. The spin expectation value has the relation  $\langle \Sigma \sigma_z \rangle = (\mu_+ + \mu_- - I)/(\mu_p + \mu_n - 1/2)$  (for notations, see Ref. [26]). The prediction was made with the single particle value of  $\langle \Sigma \sigma_z \rangle = 1$ . The spin expectation values, on the other hand, can be determined from the present experimental result, completing systematic studies on  $T = 1/2$  mirror nuclei up to  $^{43}\text{Ti}$  [27–29].

In summary, we have shown that high precision laser-microwave spectroscopy can be performed for radioactive ions produced at 1 GeV by projectile fragmentation. This guarantees that many new experiments on unexplored isotopes can follow using the same setup.

TABLE II. Nuclear magnetic moment of  $^7\text{Be}$  ( $\mu_N$ ).

Present experimental value	-1.399 28(2)
Shell model	
Cohen-Kurath (8-16)POT [20]	-1.3787
Large-basis shell model [21]	-1.132
<i>Ab initio</i> noncore shell model [22]	-1.138
Quantum Monte Carlo	
Variational quantum Monte Carlo [23]	-1.110(2)
Empirical	
Linear relations $\gamma_p = \alpha\gamma_n + \beta$ [24] <sup>a</sup>	-1.462
Isospin doublet ( $\langle \Sigma \sigma_z \rangle = 1$ )	-1.377

<sup>a</sup> $\gamma_n = \mu(^7\text{Li})/I = +3.256 462 5(4)/(3/2)$  [19] is used.

The authors thankfully acknowledge the contribution of the crew of the RIKEN Nishina Center for Accelerator-based Science for their contribution to our online experiments. This work was supported by the Grants-in-Aid for Scientific Research from the Japan Society for the Promotion Science, by the President's Special Grant of RIKEN, and by the Welch Foundation Grant No. 1546.

\*mw@riken.jp

- [1] E. W. Otten, in *Treatise on Heavy-Ion Science*, edited by D. A. Bromley (Plenum, New York, 1989), Vol. 8, p. 517.
- [2] H.-J. Kluge and W. Nörtershäuser, *Spectrochim. Acta, Part B* **58**, 1031 (2003).
- [3] M. Wada *et al.*, *Nucl. Instrum. Methods Phys. Res., Sect. B* **204**, 570 (2003).
- [4] A. Takamine *et al.*, *Rev. Sci. Instrum.* **76**, 103503 (2005).
- [5] T. Nakamura *et al.*, *Phys. Rev. A* **74**, 052503 (2006).
- [6] K. Sugimoto *et al.*, *Phys. Lett.* **18**, 38 (1965).
- [7] S. Kappertz *et al.*, in *Exotic Nuclei and Atomic Masses (ENAM 98)*, edited by B. M. Sherrill, D. J. Morrissey, and C. N. David (AIP, New York, 1998), Vol. 455, p. 110.
- [8] A. Bohr and V. F. Weisskopf, *Phys. Rev.* **77**, 94 (1950).
- [9] T. Fujita, K. Ito, and T. Suzuki, *Phys. Rev. C* **59**, 210 (1999).
- [10] Z.-C. Yan, D. K. McKenzie, and G. W. F. Drake, *Phys. Rev. A* **54**, 1322 (1996).
- [11] V. A. Yerokhin, *Phys. Rev. A* **77**, 020501(R) (2008).
- [12] D. J. Wineland, W. M. Itano, and R. S. Van Dyck, Jr., *Adv. At. Mol. Phys.* **19**, 135 (1983).
- [13] K. Okada *et al.*, *J. Phys. Soc. Jpn.* **67**, 3073 (1998).
- [14] T. Nakamura *et al.*, *Opt. Commun.* **205**, 329 (2002).
- [15] T. Kubo *et al.*, *Nucl. Instrum. Methods Phys. Res., Sect. B* **70**, 309 (1992).
- [16] T. Udem, R. Holzwarth, and T. W. Haensch, *Nature (London)* **416**, 233 (2002).
- [17] F. Diedrich, E. Peik, J. M. Chen, W. Quint, and H. Walther, *Phys. Rev. Lett.* **59**, 2931 (1987).
- [18] W. M. Itano, *Phys. Rev. B* **27**, 1906 (1983).
- [19] N. J. Stone, *At. Data Nucl. Data Tables* **90**, 75 (2005).
- [20] S. Cohen and D. Kurath, *Nucl. Phys.* **73**, 1 (1965).
- [21] P. Navrátil and B. R. Barrett, *Phys. Rev. C* **57**, 3119 (1998).
- [22] P. Navrátil and W. E. Ormand, *Phys. Rev. C* **68**, 034305 (2003).
- [23] B. S. Pudliner, V. R. Pandharipande, J. Carlson, S. C. Pieper, and R. B. Wiringa, *Phys. Rev. C* **56**, 1720 (1997).
- [24] B. Buck, A. C. Merchant, and S. M. Perez, *Phys. Rev. C* **63**, 037301 (2001).
- [25] R. Schiavilla, V. R. Pandharipande, and D. O. Riska, *Phys. Rev. C* **40**, 2294 (1989).
- [26] K. Sugimoto, *Phys. Rev.* **182**, 1051 (1969).
- [27] S. S. Hanna and J. W. Hugg, *Hyperfine Interact.* **21**, 59 (1985).
- [28] M. Fukuda *et al.*, *Phys. Lett. B* **307**, 278 (1993).
- [29] W. F. Rogers, D. L. Clark, S. B. Dutta, and A. G. Martin, *Phys. Lett. B* **177**, 293 (1986).